

Supporting Information for:

Syringe Injectable Electronics: Precise Targeted Delivery with Quantitative Input/Output Connectivity

*Guosong Hong, Tian-Ming Fu, Tao Zhou, Thomas G. Schuhmann, Jinlin Huang and Charles M. Lieber**

This file includes:

Materials and Methods

Supplementary Figures S1-S5

Supplementary Video Captions S1-S3

Supplementary References

Materials and Methods

Fabrication of Injectable Mesh Electronics.

The geometrical design of injectable mesh electronics is similar to our recent report,¹ with its key parameters as follows: total width $W = 4$ mm, longitudinal ribbon width $w_1 = 20$ μm , transverse ribbon width $w_2 = 20$ μm , angle between longitudinal and transverse ribbons $\alpha = 45^\circ$, longitudinal spacing $L_1 = 333$ μm , transverse spacing $L_2 = 250$ μm , metal interconnect line width $w_m = 10$ μm and total number of channels $N = 16$. Key steps used in the fabrication of the mesh electronics are given as follows:¹ (i) A 100 nm layer of Ni, which was used as the sacrificial layer, was thermally evaporated (Sharon Vacuum, Brockton, MA) onto the pre-cleaned Si wafer (n-type 0.005 $\Omega\text{-cm}$, 600-nm thermal oxide, Nova Electronic Materials, Flower Mound, TX). (ii) The Si wafer was spin-coated with 500 nm negative photoresist SU-8 (SU-8 2000.5; MicroChem Corp., Newton, MA) and pre-baked at 65 $^\circ\text{C}$ on a hot plate for 1 min and then transferred to a 95 $^\circ\text{C}$ hot plate for 4 min, before photolithography (PL) patterning (ABM mask aligner, San Jose, CA). The exposed SU-8 photoresist was post-baked at 65 $^\circ\text{C}$ for 3 min and 95 $^\circ\text{C}$ for 3 min. (iii) After post-baking, the SU-8 photoresist was developed (SU-8 Developer, MicroChem Corp., Newton, MA) for 2 min, rinsed with isopropanol, and hard-baked at 185 $^\circ\text{C}$ for 1 h. (iv) Subsequently, the wafer was spin-coated with MCC Primer 80/20 and LOR 3A lift-off resist (MicroChem Corp., Newton, MA), and baked at 185 $^\circ\text{C}$ for 5 min, followed by spin-coating Shipley 1805 photoresist (Microposit, The Dow Chemical Company, Marlborough, MA), which was baked at 115 $^\circ\text{C}$ for 5 min. The resist was patterned by PL and developed (MF-CD-26, Microposit, The Dow Chemical Company, Marlborough, MA) for 90 s. (v) A 1.5-nm Cr layer and a 100-nm thick Au layer were deposited by electron-beam evaporation (Denton Vacuum, Moorestown, NJ) followed by lift-off (Remover PG, MicroChem Corp., Newton, MA). (vi) Steps *iv* and *v* were repeated for lithographically patterning and depositing the Pt sensing electrodes (Cr: 1.5 nm, Pt: 50 nm). (vii) Steps *ii* and *iii* were repeated for lithographically patterning the top SU-8 layer, which serves as the top encapsulating/passivating layer. (viii) The Si wafer with fabricated mesh electronics was transferred to a Ni etchant solution comprising 40% FeCl_3 :39% HCl : $\text{H}_2\text{O} = 1:1:20$ to release the mesh electronics from the fabrication substrate. Released mesh structures were rinsed with deionized (DI) water, transferred to an aqueous solution of poly-D-lysine (PDL, 1.0 mg/ml, MW 70,000-150,000, Sigma-Aldrich Corp., St. Louis, MO) for 24-48 h,

and then transferred to 1X phosphate buffered saline (PBS) solution (HyClone™ Phosphate Buffered Saline, Thermo Fisher Scientific Inc., Pittsburgh, PA).

Controllable Injection into Dense Materials and Biological Tissues.

Loading Injectable Mesh Electronics into Glass Needles.

Glass capillary needles (Drummond Scientific Co., Broomall, PA.) with inner diameter (I.D.) of 400 μm and outer diameter (O.D.) of 650 μm were used for injection tests. To load the free-standing mesh electronics, the glass needle was inserted in a micropipette holder (Q series holder, Harvard Apparatus, Holliston, MA), which was connected to a 1-mL syringe (NORM-JECT®, Henke Sass Wolf, Tuttlingen, Germany) through an Intramedic™ polyethylene catheter tubing (I.D. 1.19 mm, O.D. 1.70 mm, Becton Dickinson and Company, Franklin Lakes, NJ). The syringe was used to manually draw the mesh electronics into the glass needle.

Preparation of Hydrogel.

0.5 g agarose (SeaPlaque® Lonza Group Ltd., Basel, Switzerland) was mixed with 100 mL DI water in a glass beaker. The beaker was covered with a piece of aluminum foil (Reynolds Wrap® Reynolds Consumer Products, Lake Forest, Illinois) to prevent evaporation and heated at boiling on a hot plate until the solution was clear; the final mass concentration was ca. 0.5%. The solution was allowed to naturally cool to room temperature where it exists as a hydrogel with mechanical properties similar to those of dense brain tissue.²⁻⁶

Vertebrate Animal Subjects.

Adult (25-35 g) male C57BL/6J mice (Jackson Laboratory, Bar Harbor, ME) were used as vertebrate animal subjects in this study. All procedures performed on the vertebrate animal subjects were approved by the Animal Care and Use Committee of Harvard University. The animal care and use programs at Harvard University meet the requirements of the Federal Law (89-544 and 91-579) and NIH regulations and are also accredited by the American Association for Accreditation of Laboratory Animal Care (AAALAC). Animals were group-housed on a 12 h:

12 h light: dark cycle in the Harvard University's Biology Research Infrastructure (BRI) and fed with food and water *ad libitum* as appropriate.

Preparation of Ex Vivo Mouse Brains.

C57BL/6J mice were euthanized via intraperitoneal injection of Euthasol (Virbac Corporation, Fort Worth, TX) at a dose of 270 mg/kg body weight in accordance with the recommendations of the Panel on Euthanasia of the American Veterinary Medical Association.⁷ After euthanasia, mice were decapitated and brains were removed from the skull and placed in 4% formaldehyde for 24 h for fixation. Excess formaldehyde was removed by rinsing the fixed brain in 1X PBS for 24 h and the brain tissue was stored in fresh 1X PBS solution before controlled mesh electronics injection tests.

Controlled Injection of Mesh Electronics into Hydrogel and Ex Vivo Mice Brains.

Either 0.5% agarose hydrogel as a brain tissue mimic or the *ex vivo* fixed brain tissue was placed in a petri dish. The glass needle loaded with mesh electronics was inserted in the micropipette holder, which was connected to a 5 mL syringe (Becton Dickinson and Company, Franklin Lakes, NJ) through an IntramedicTM polyethylene catheter tubing (I.D. 1.19 mm, O.D. 1.70 mm). The 5 mL syringe was pre-filled with 1X PBS and mounted on a syringe pump (PHD 2000, Harvard Apparatus, Holliston, MA). The micropipette holder was mounted on a stereotaxic stage equipped with a motorized linear translation stage (860A motorizer and 460A linear stage, Newport Corporation, Irvine, CA) that could move the stereotaxic arm in *z* direction with constant preset velocity ranging from 0.05 to 0.5 mm/s. The needle was positioned at the surface of the 0.5% hydrogel or the *ex vivo* fixed mouse brain samples, and liquid was injected through the mesh-loaded glass needle at a volumetric flow rate of 10 ml/h to expel air bubbles from the entire injection system. The needle was then inserted into the injection medium to the desired depth and x-y coordinates. Controlled injection was carried out by synchronizing the syringe pump with the motorized linear translation stage, with a typical liquid injection rate of 20-50 mL/h and a typical translational stage retraction velocity of 0.2-0.5 mm/s. In the field of view (FoV) method, the liquid injection rate and the needle retraction velocity were independently adjusted such that the upper part of the mesh electronics, which was visualized through an eyepiece camera (DCC1240C, Thorlabs Inc., Newton, NJ), remained stationary in the FoV of the

camera. The optimum volumetric flow rate and the needle retraction rate were determined through experimental optimization to achieve fully extended mesh morphology with minimum motion relative to the injected medium, and a general rule of thumb dictates that a greater volumetric flow rate is needed for wider and thicker mesh designs, smaller needle diameter and higher needle retraction rate. Typical solution volumes injected into the medium with 4 mm length mesh were 10-100 μL , on the same order of magnitude as the volume of liquid introduced during intracranial injection of virus vectors and enzymes in saline and artificial cerebrospinal fluid into rodent brain (ranging from 1~100 μL).⁸⁻¹¹ After the glass needle was fully retracted from the injection medium, the volumetric liquid injection rate was increased to 100 mL/h to fully expel the mesh electronics from the needle onto the outer surface of the injection medium or a support used for making input/output (I/O) connections for external recording instruments. The extended morphology of the mesh in 0.5% hydrogel was verified by lowering the eyepiece camera to cover the lower part of the mesh electronics inside the transparent hydrogel. The targeting precision was estimated by tracking the motion of the bottom end of mesh electronics during the injection process using the same eyepiece camera, which had a pixel resolution of ca. 4.2 μm . For *ex vivo* brain tissue, the morphology of the injected mesh was verified by micro-computed tomography (micro-CT) given the optical opacity of the tissue.

Controlled In Vivo Injection of Mesh Electronics into Mice Brains.

For *in vivo* injection experiments, all metal tools in direct contact with the mice were autoclaved for 1 h and all plastic tools in direct contact with the mice were sterilized with 70% ethanol and rinsed with sterile DI water and sterile 1X PBS before use. Mesh electronic samples were sterilized by 70% ethanol followed by rinsing with sterile DI water and transferring to sterile 1X PBS. C57BL/6J mice were anesthetized by intraperitoneal injection of a mixture of 75 mg/kg of ketamine (Patterson Veterinary Supply Inc., Chicago, IL) and 1 mg/kg dexdomitor (Orion Corporation, Espoo, Finland). A heating pad (Harvard Apparatus, Holliston, MA) was set to 37°C and placed underneath the mouse to maintain body temperature. The depth of anesthesia was monitored via the toe pinch method.¹² In a given experiment, a mouse was placed in the stereotaxic frame (Lab Standard Stereotaxic Instrument, Stoelting Co., Wood Dale, IL) with two ear bars and one nose clamp used to fix the head in position. Hair removal lotion (Nair®, Church & Dwight, Ewing, NJ) was used for depilation over the mouse head and iodophor was applied to

sterilize the depilated scalp skin. A 5-mm longitudinal incision was made in the scalp, and the scalp skin was resected over the sagittal sinus of the skull, exposing a 1 cm × 1 cm portion of the skull. Two 0.5-mm diameter burr holes were drilled using a dental drill (Micromotor with On/Off Pedal 110/220, Grobet USA, Carlstadt, NJ) according to the following stereotaxic coordinates: left burr hole: anteroposterior: -1.20 mm, mediolateral: -1.25 mm; right burr hole: anteroposterior: -1.20 mm, mediolateral: +2.45 mm. The dura was carefully incised and resected using a 27-gauge needle (PrecisionGlide®, Becton Dickinson and Company, Franklin Lakes, NJ). Sterile 1X PBS was swabbed on the surface of the brain to keep it moist throughout the surgery. The same injection process as described in “Controlled Injection of Mesh Electronics into Hydrogel and Ex Vivo Mice Brains” was used for injection of mesh electronics into the live mouse brain through the two burr holes. Typical solution volumes injected into the brain with 4 mm length mesh were 10-100 μ L. After the two injections, the mice were euthanized via intraperitoneal injection of Euthasol at a dose of 270 mg/kg body weight and decapitated. The mouse head was fixed on a user-made stage for micro-CT imaging.

Micro-Computed Tomography.

The morphologies of injected mesh electronics in opaque *ex vivo* brain tissue and decapitated mouse head after *in vivo* injection were imaged using an HMXST Micro-CT X-ray scanning system with a standard horizontal imaging axis cabinet (model: HMXST225, Nikon Metrology, Inc., Brighton, MI). Typical imaging parameters were 80 kV and 121 μ A (no filter) for scanning the *ex vivo* brain tissue, and 115 kV and 83 μ A (with a 0.1-mm copper filter for beam hardening) for scanning the decapitated mouse head with cranial bones. In both cases, shading correction and flux normalization were applied before scanning to adjust the X-ray detector. The *CT Pro 3D* software (ver. 2.2, Nikon-Metris, UK) was used to calibrate centers of rotation for micro-CT sinograms and to reconstruct the images. *VGStudio MAX* software (ver. 2.2, Volume Graphics GmbH, Germany) was used for 3D rendering and analysis of the reconstructed images. False colors were added using the *VGStudio MAX* software to differentiate the soft tissue, bones and the metal interconnect lines in the mesh electronics due to their different contrasts to X-ray.

Implementation and Characterization of High-Yield I/O Bonding.

Preparation of Conductive Ink.

Carbon nanotubes (Stock No.: P093099-11, Tubes@Rice, Houston, TX) were received as a slurry in toluene. The toluene was evaporated at 100 °C on a hot plate to carbon nanotube powders. 100 mg of carbon nanotube powder and 400 mg of sodium dodecylbenzenesulfonate (Sigma-Aldrich Corp., St. Louis, MO) were mixed with 4 mL DI water. The mixture was sonicated using a bath sonicator (Crest Ultrasonics Corp., Model 500D, Trenton, NJ) for 1 h at its maximum power (power setting = 9, power = 120 W) with replacement of the sonication bath every 20 min to maintain a bath temperature < 40 °C. Following sonication the concentrated carbon nanotube suspension could be stored at room temperature for 3 months without significant precipitation. A brief, 5-min sonication at power setting of 9 was performed immediately prior to using as a conductive ink for I/O bonding.

I/O Bonding by Conductive Ink Printing.

The carbon nanotube-based conductive ink was loaded into pulled glass capillary tube (I.D. 400 µm, O.D. 650 µm), which serves as the printer head. After pulling (Model P-97, Sutter Instrument, CA), the tapered tip of the glass capillary tube was ground to yield the optimal 150 µm I.D.. The printer head was fixed with an electrode holder (Warner Instruments, Hamden, CT) and dipped into the freshly sonicated carbon nanotube conductive ink; capillary forces draw the conductive ink to height of ca. 1 cm in the printer head. The ink-loaded printer head was mounted onto a motorized micromanipulator (MP-285/M, Sutter Instrument, Novato, CA) controlled by a rotary optical encoder (ROE-200, Sutter Instrument, Novato, CA) and controller (MPC-200, Sutter Instrument, Novato, CA). After the I/O part of the mesh electronics was unfolded and dried to expose all I/O pads on a 16-channel flexible flat cable (FFC, PREMO-FLEX, Molex Incorporated, Lisle, IL), a user-written LabVIEW program was used to take the desired start position (the position of the mesh I/O pad) and end position (the position of the electrode in the FFC cable) for each channel as input coordinates and compute the minimum path between the two positions. Then the LabVIEW program drove the printer head to print the conductive ink along each computed path automatically in a ‘hopping’ motion with a typical step size of 150 µm. After the 16 independent connections (between mesh I/O pads and FFC cable lines) each channel of the mesh electronics could be individually addressed.

Resistance Characterization of I/O Connections Using Conductive Ink.

Multiple 5 mm lines were printed using the above method with widths between 80 and 300 μm . The resistance of each line was characterized using four-point probe resistance measurement with the inner two probes recording the voltage and the outer two recording the current on an Agilent 4156C semiconductor parameter analyzer (Agilent Technologies Inc., Santa Clara, CA) to minimize contact resistances.

I/O Bonding Using Anisotropic Conductive Film (ACF).

The I/O part of the mesh electronics was unfolded and dried on a glass slide to expose all I/O pads. A piece of ACF (CP-13341-18AA, Dexerials America Corporation, San Jose, CA) with a length of 15 mm and width of 1.5 mm was placed over the I/O pads and partially bonded at 75 $^{\circ}\text{C}$ and 1 MPa for 10 s using a commercial flip-chip bonder (Fineplacer Lambda Manual Sub-Micron Flip-Chip Bonder, Finetech, Inc., Manchester, NH). Then an FFC cable was placed on top of the ACF, aligned with the mesh I/O pads and bonded at 165-200 $^{\circ}\text{C}$ and 4 MPa for 1-2 min.

Noise Spectrum Characterization of I/O Connections.

The sensing electrodes of two identical sets of mesh electronics were immersed in 1X PBS and their I/O pads bonded using either the conductive ink printing or ACF methods. The FFC cable, which was bonded to the mesh I/O pads, was connected to an Intan RHD 2132 amplifier evaluation system (Intan Technologies LLC., Los Angeles, CA) through a home-made printed circuit board (PCB). Ag/AgCl electrode was used as a reference. For noise evaluation, electrical recording measurements were made with a 20-kHz sampling rate and a 60-Hz notch filter. The recorded traces were analyzed, and corresponding noise-power spectra were plotted after fast Fourier transform (Figure 4D).

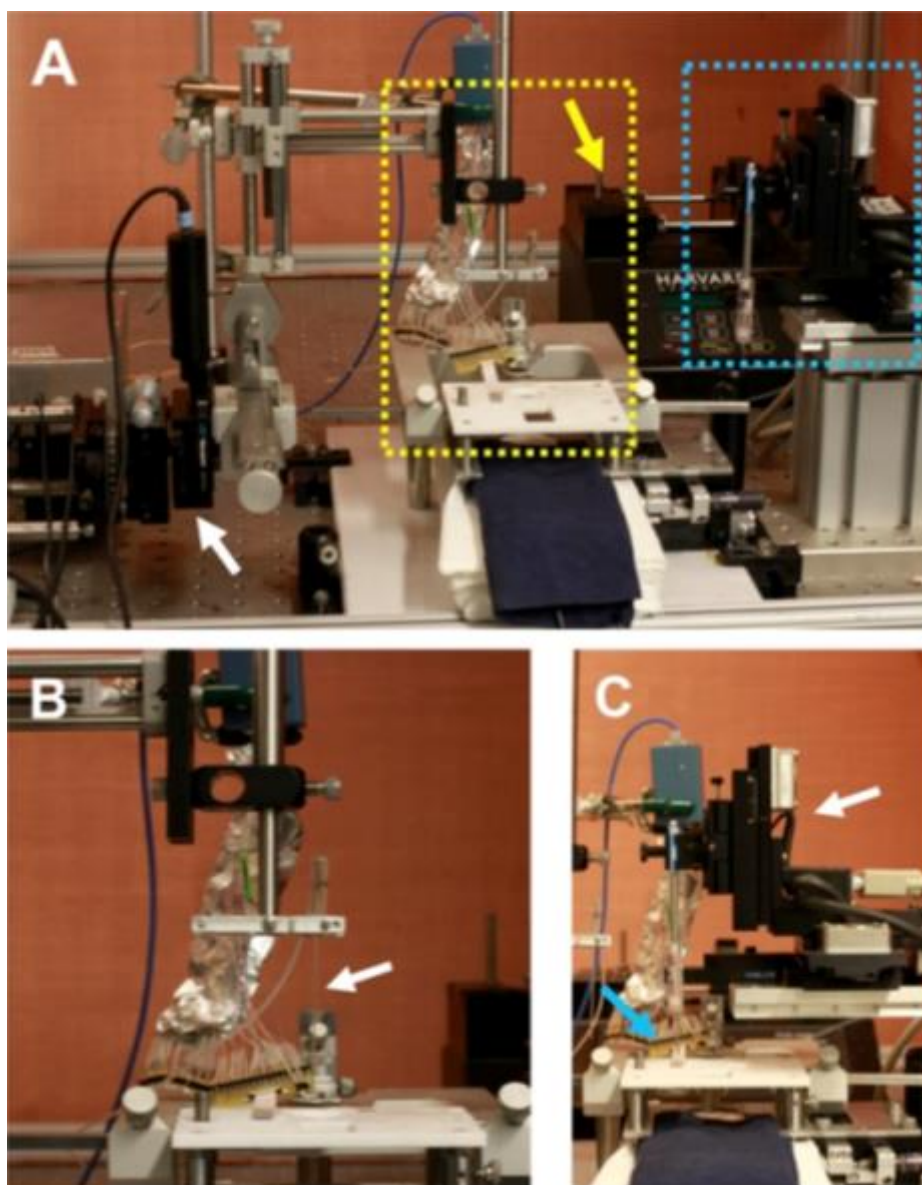


Figure S1. Experimental mesh injection and I/O bonding set-ups. (A) Overview of the entire setup showing the relevant instrumentation for controlled injection (yellow dashed box) and conductive ink printing (blue dashed box). The yellow arrow indicates the syringe pump used for controlling the volumetric liquid injection rate, and the white arrow highlights the linear translational motor that drives the stereotaxic stage. (B) Zoomed-in view of the controlled injection setup, where the white arrow indicates the glass needle loaded with mesh electronics for injection. (C) Zoomed-in view of the conductive ink printing setup, where the white arrow indicates the motorized and computerized micromanipulator, and the blue arrow indicates the printer head loaded with conductive ink.

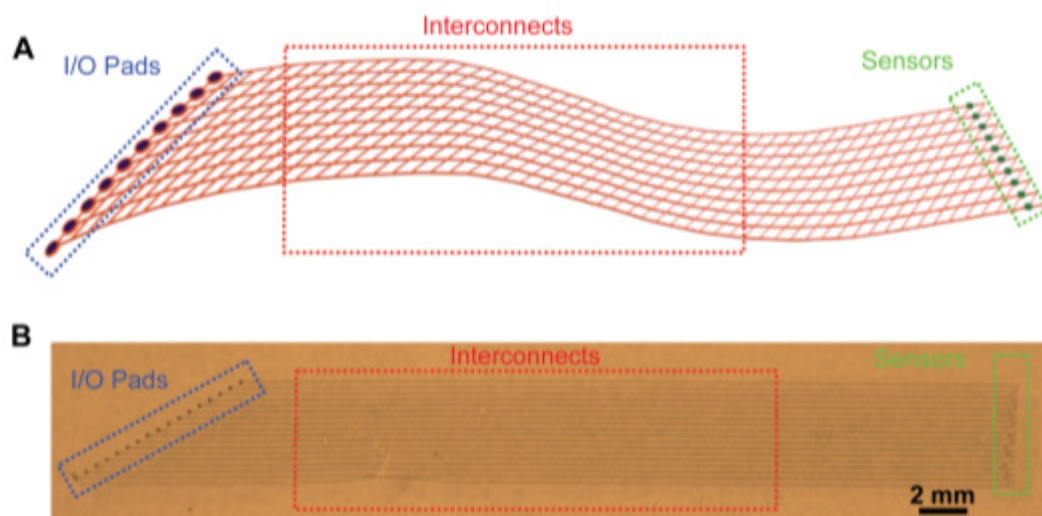


Figure S2. Structure of syringe-injectable mesh electronics. (A) Schematic of the mesh electronics structure, where the red network corresponds to SU-8 polymer, which defines the overall mesh structure and encapsulates the metal interconnect lines in the three-layer SU-8/metal/SU-8 structure, the green dashed box highlights the sensor electrodes (dark green dots), the red dashed box highlights the metal interconnect lines, and the blue dashed box highlights the I/O pads (dark blue circles). (B) Optical image of a fabricated mesh electronics probe, where the green, red and blue dashed boxes highlight the sensor electrodes, the metal interconnects and the I/O pads, respectively, as in (A).

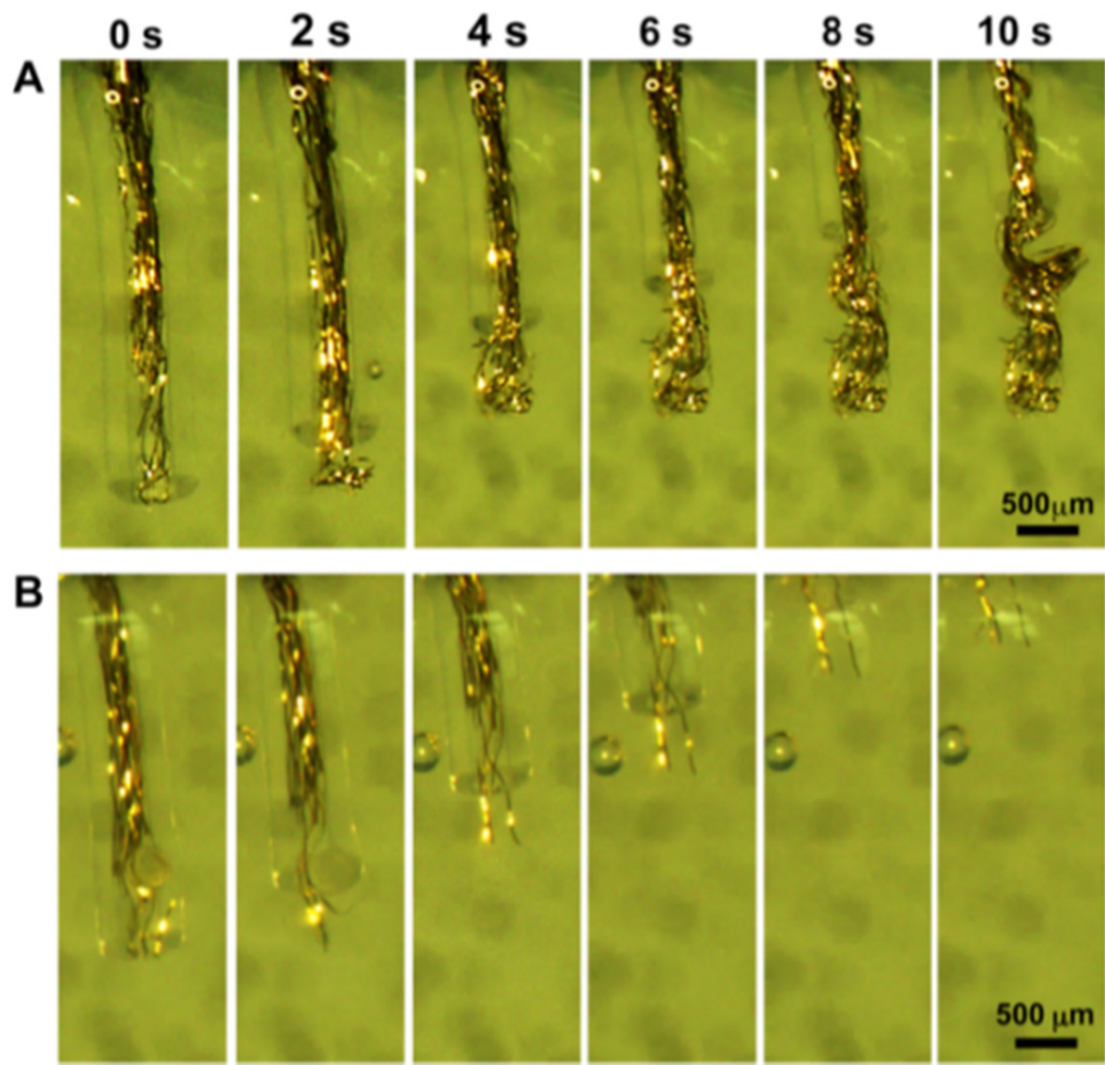


Figure S3. Injection processes with mismatched injection rate and needle retraction speed. (A) Time course white-light optical photographs of the mesh electronics injection process when the needle is withdrawn at a speed slower than the injection rate, resulting in crumpled mesh electronics structure and inaccurate delivery of mesh electrodes into the medium. (B) Time course photos of the mesh electronics injection process when the needle is withdrawn at a speed faster than the injection rate, resulting in partial withdrawal of the mesh electronics structure from the medium. In (A) and (B) the medium was 0.5% (wt/vol %) agarose hydrogel.

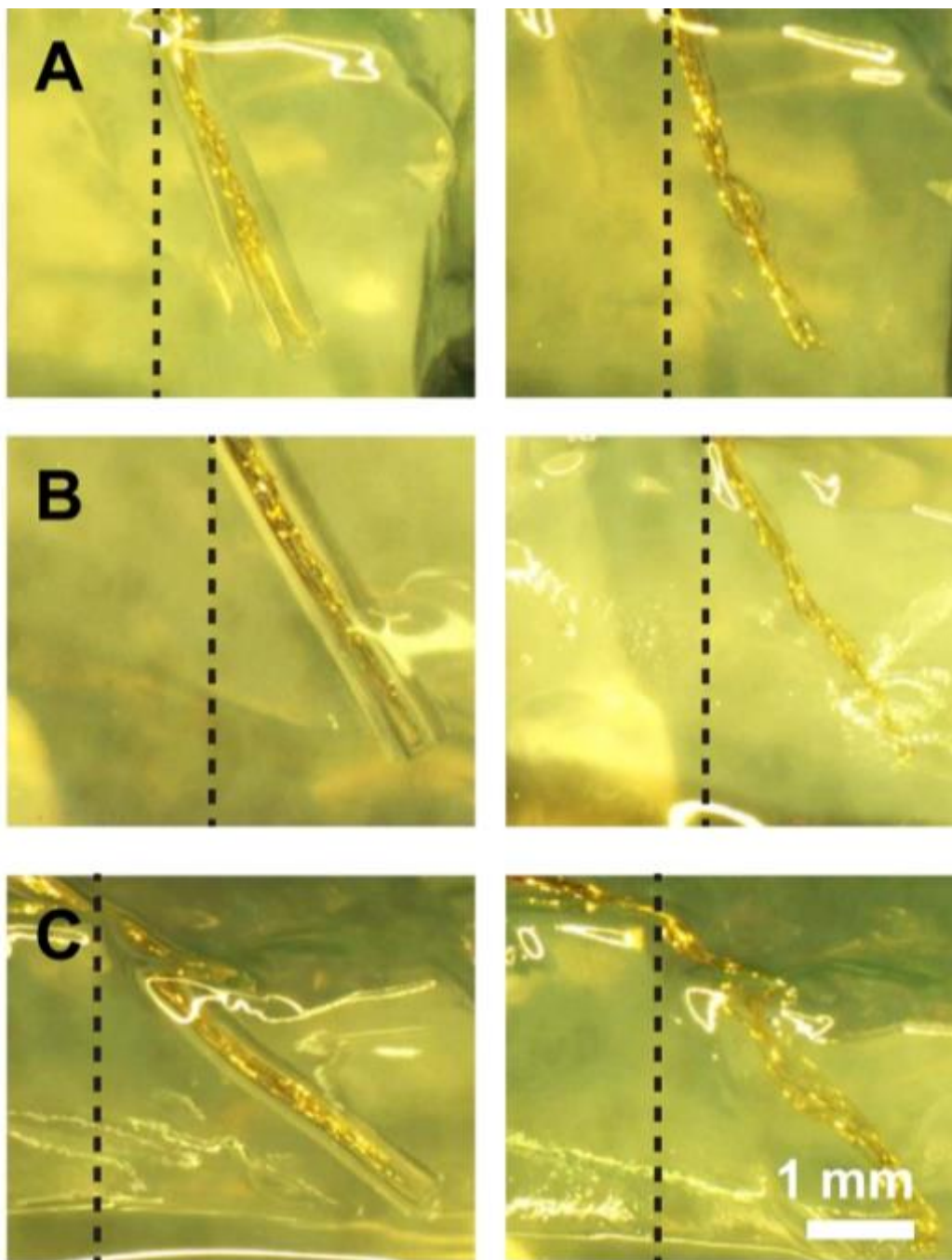


Figure S4. Controlled injection of mesh electronics at different angles. White-light optical photographs are shown for controlled injections of mesh electronics at 15° (A), 30° (B) and 45° (C) to normal direction (black dashed lines) before (left) and after (right) injection. The medium in all of the experiments was 0.5% (wt/vol %) agarose hydrogel.

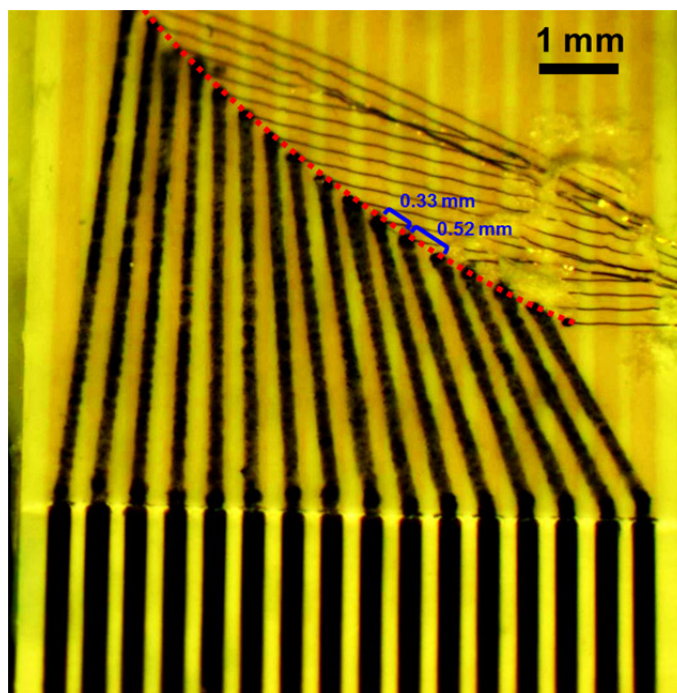


Figure S5. Conductive ink printing method provides 100% connectivity for a mesh electronics with imperfectly unfolded mesh I/O pads. The mesh I/O pads are spatially distributed in a curve (red dashed line) with varying distances between neighboring pads (two examples of inter-pad distances labeled in blue). It is straightforward to bridge these I/O pads to the regular pitch lines on the FFC cable (dark vertical lines, lower quarter of image) using the conductive CNT ink printing method. In contrast, it would not be possible to connect all of the I/O pads bonded to the FFC using the ACF bonding method reported previously.¹

Supplementary Videos

Video S1. Field of view (FoV) controlled injection into hydrogel. This video shows the motions of the I/O end of the mesh electronics and the glass needle with respect to a fixed camera FoV during the injection process. At the end of the injection the camera FoV was moved to the sensor end of the mesh electronics inside the transparent hydrogel. The frame rate is 15 frames per second (fps) and the video is played at 3× real time.

Video S2. Controlled injection obtained by monitoring the mesh end inside the hydrogel. This video shows the motion of the sensor end of the mesh electronics and the glass needle visualized through the transparent hydrogel during the injection process. The frame rate is 15 fps and the video is played at 3× real time.

Video S3. Automated conductive ink printing of I/O connections. This video shows the printer head, which is made from a tapered glass capillary tube and loaded with carbon nanotube ink, printing continuous conductive lines under hands-free computer control to electrically connect the individual I/O pads of the mesh electronics to corresponding channel lines of the FFC cable. The frame rate is 15 fps and the video is played at 4× real time.

Supplementary References

1. Liu, J.; Fu, T.-M.; Cheng, Z. G.; Hong, G. S.; Zhou, T.; Jin, L. H.; Duvvuri, M.; Jiang, Z.; Kruskal, P.; Xie, C.; Suo, Z. G.; Fang, Y.; Lieber, C. M. *Nat. Nanotechnol.* **2015**, *10*, 629-636.
2. Chen, Z. J.; Gillies, G. T.; Broaddus, W. C.; Prabhu, S. S.; Fillmore, H.; Mitchell, R. M.; Corwin, F. D.; Fatouros, P. P. *J. Neurosurg.* **2004**, *101*, 314-322.
3. Ahearne, M.; Yang, Y.; El Haj, A. J.; Then, K. Y.; Liu, K. K. *J. R. Soc. Interface* **2005**, *2*, 455-463.
4. Chen, X. M.; Sarntinoranont, M. *Ann. Biomed. Eng.* **2007**, *35*, 2145-2158.
5. Deepthi, R.; Bhargavi, R.; Jagadeesh, K.; Vijaya, M. S. *SAS Tech Journal* **2010**, *9*, 27-30.
6. Pervin, F.; Chen, W. W., Mechanically similar gel simulants for brain tissues. In *Dynamic Behavior of Materials, Volume 1*, Springer: 2011; pp 9-13.
7. Leary, S.; Underwood, W.; Anthony, R.; Cartner, S.; Corey, D.; Grandin, T.; Greenacre, C. B.; Gwaltney-Bran, S.; McCrackin, M. A.; Meyer, R. *American Veterinary Medical Association* **2013**.
8. Xue, M. Z.; Hollenberg, M. D.; Yong, V. W. *J. Neurosci.* **2006**, *26*, 10281-10291.
9. Brian, J. E.; Moore, S. A.; Faraci, F. M. *Stroke* **1998**, *29*, 2600-2605.
10. Shen, J., *Factors Influencing Topotecan CNS Penetration in Mouse Models*. ProQuest: 2008.
11. Huang, C. C.; Liu, C. C.; Wang, S. T.; Chang, Y. C.; Yang, H. B.; Yeh, T. F. *Pediatr. Res.* **1999**, *45*, 120-127.
12. Collier, H. O.; Skerry, R.; Warner, B. T. *Brit. J. Pharm. Chemoth.* **1961**, *17*, 28-40.